

BASE 04
515001380727

IFUSP/P-12

MAGNETO-ACOUSTIC ATTENUATION IN AuSb_2 *

by

B.I.F. - USP

F.P.Missell, J.M.V.Martins, C.C.Becerra,
N.S. Wisnik and Y.Shapira**

Instituto de Física, Universidade de São Paulo

* Work supported by Fundação de Amparo à Pesquisa do Estado de São Paulo, Banco Nacional de Desenvolvimento Econômico e Conselho Nacional de Pesquisas.

** On leave from Francis Bitter National Magnet Laboratory M.I.T. Cambridge, Massachusetts, USA.

Submitted to: The Journal of Physics and Chemistry of Solids.

November/1973

ABSTRACT

MAGNETO-ACOUSTIC ATTENUATION IN AuSb_2

Quantum oscillations in the ultrasonic attenuation in AuSb_2 , were studied as a function of temperature, magnetic field and crystal orientation. The effective masses of the carriers associated with the F_5 and F_6 oscillations were measured in a (110) plane. For the F_5 oscillations, the Dingle temperature and apparent magnetic breakdown field appear to depend strongly upon orientation. For the F_6 oscillations, however, there were no signs of magnetic breakdown up to the highest magnetic fields available (70 kOe) and the Dingle temperature was roughly independent of orientation. From the acoustic velocities, the elastic constants were determined at 77 K: $C_{11} = (14.7 \pm 0.9) \times 10^{11}$ dyne/cm², $C_{12} = (6.0 \pm 0.9) \times 10^{11}$ dyne/cm², and $C_{44} = (2.59 \pm 0.06) \times 10^{11}$ dyne/cm². These elastic constants give an adiabatic compressibility $K_S = (1.13 \pm 0.12) \times 10^{-12}$ cm²/dyne and a Debye temperature $\theta_D = (203 \pm 15)$ K.

MAGNETO-ACOUSTIC ATTENUATION IN AuSb_2 INTRODUCTION

In recent years, there has been a considerable interest in applying experimental techniques such as the de Haas-van Alphen (dHvA) effect and magnetoresistance measurements to the study of metallic compounds. With the realization that sufficiently pure samples of these materials could be prepared, a growing effort has been made to understand the electronic structure of this class of solids, whose chemical binding forces cannot be clearly classified as ionic, metallic or covalent. In this light, the compound AuSb_2 has been studied previously by means of transport measurements¹⁻⁴ and by the dHvA effect.⁵⁻⁷ The previously successful applications of the nearly free-electron (NFE) model as a first approximation to the Fermi surface of certain metallic compounds,⁸ led Ahn and Sellmyer^{6,7} to compare this model with their extensive measurements of the dHvA frequencies in AuSb_2 . They concluded, however, that the NFE model was not a good approximation to the Fermi surface of AuSb_2 . In the present study, measurements of the ultrasonic attenuation were used to determine the dHvA frequencies of AuSb_2 and the effective masses as a function of orientation.

EXPERIMENT

Measurements of the ultrasonic attenuation were

made using conventional pulse-echo techniques⁹. The transducers were X and Y-cut quartz with a ~ 10 MHz fundamental frequency. The ultrasonic attenuation was measured near the fundamental frequency and the first two odd harmonics. Acoustical bonds were made with Dow Corning 200 silicone oil, having a viscosity of 30 000 centistoke at 25°C. The round trip transit time of the acoustical pulse in the sample was determined from the separation of the echos on an oscilloscope whose time base had been calibrated with a Tektronix Time Mark Generator. The acoustic velocities were then determined, after an estimated correction for thermal contraction.

The sample used in these experiments was spark cut from a single crystal, kindly provided by Prof. D.J. Sellmyer. It had the shape of a half-cylinder with the $[110]$ crystal axis along the cylinder axis. A Laue photograph indicated that the $[110]$ axis coincided with the cylinder axis to within 1°. However, the final orientation of the crystal axes with respect to the magnetic field had an uncertainty of 2°-3°. Magnetic fields of up to 70 kOe were generated by a high-homogeneity superconducting solenoid. Sample temperatures were determined from the pressure over the helium bath in which the sample was immersed.

RESULTS AND DISCUSSION

A. Sound Velocities and Elastic Constants

The pyrite crystal structure of AuSb_2 can be

considered as an NaCl-like grouping of gold atoms and Sb_2 pairs.¹⁰ Thus, AuSb_2 is cubic and its elastic properties are determined by three elastic constants: C_{11} , C_{12} , and C_{44} . These three elastic constants may be determined from the three acoustic velocities for sound propagation along the $[110]$ axis. For a temperature of 77K, we found

$$v_L = (3.59 \pm 0.1) \times 10^5 \text{ cm/sec}, \quad \vec{\alpha} \parallel \vec{\xi} \parallel [110]$$

$$v_{T1} = (2.08 \pm 0.04) \times 10^5 \text{ cm/sec}, \quad \vec{\alpha} \parallel [110], \vec{\xi} \parallel [1\bar{1}0]$$

$$v_{T2} = (1.61 \pm 0.02) \times 10^5 \text{ cm/sec}, \quad \vec{\alpha} \parallel [110], \vec{\xi} \parallel [001]$$

where $\vec{\alpha}$ is the wave vector of the sound wave and $\vec{\xi}$ is the particle displacement. To determine the elastic constants, the density was calculated from the room temperature lattice constant,¹ $a = 6.658 \text{ \AA}$, and a correction for thermal contraction was estimated. In this manner, we found: $C_{11} = (14.7 \pm 0.9) \times 10^{11} \text{ dyne/cm}^2$, $C_{12} = (6.0 \pm 0.9) \times 10^{11} \text{ dyne/cm}^2$, and $C_{44} = (2.59 \pm 0.06) \times 10^{11} \text{ dyne/cm}^2$. Using these values for the elastic constants, the adiabatic compressibility is $K_S = 3/(C_{11} + 2C_{12}) = (1.13 \pm 0.12) \times 10^{-12} \text{ cm}^2/\text{dyne}$. Using de Launay's method,¹¹ the Debye temperature was found to be $\theta_D = (203 \pm 15) \text{ K}$. Since there has been a certain amount of confusion in the literature over the definition of θ_D ,¹² we note that in the Debye model the lattice contribution to the specific heat at $T \ll \theta_D$ is given by

$$C_L = 1944 n(T/\theta_D)^3 \text{ joules/mole-degree}$$

where n is the number of atoms per molecule ($n=3$ for AuSb_2).¹³ The above value for θ_D is for a triatomic solid. The velocities V_L and V_{T2} were also measured at 4.2 K and were found to have changed by less than 2% from their values at 77 K. This result suggests that the elastic constants do not depend strongly on temperature between 4.2 K and 77 K and, therefore, the above value of θ_D is approximately equal to θ_D at $T=0$

B. dHvA Frequencies

The dHvA frequencies were measured as a function of crystal orientation for the magnetic field in a (110) plane. The frequencies F_5 and F_6 (notation of ref.6) were strongly present in the attenuation and were observed over the same angular range as in ref. 6. The values of these frequencies were also in good agreement with those measured in ref. 6. The frequency F_1 was observed for angles very close to the [110] direction, but could not be followed over the angular range for which it was observed in ref. 6. Similarly, the frequency F_7 was observed up to 30° from the $[\bar{1}\bar{1}0]$ axis, but could not be observed for large angles.

In Fig. 1, a typical experimental curve is shown, for 12.1 MHz longitudinal sound waves propagating along a [110] axis. The magnetic field is in the plane perpendicular to the direction of sound propagation, at an angle of 30° from the $[\bar{1}\bar{1}0]$ axis. The sample temperature is 4.15 K. The high frequency oscillations are associated with F_5 , while

the low frequency oscillations correspond to F_7 .

C. Temperature Dependence of the Amplitudes

Since the F_5 and F_6 oscillations were large and easily observable over a wide angular range, it was possible to study the cyclotron effective masses associated with these carrier pockets in some detail. Cyclotron masses were determined in the standard way, from the temperature dependence of the amplitude at constant magnetic field.^{14,15} In Fig. 2, a plot of $\ln \left\{ \frac{A}{T} \left[1 - \exp \left(- \frac{4\pi^2 kT}{\hbar\omega_c} \right) \right] \right\}$ vs. T is shown for

the amplitude A associated with the F_5 oscillations. The magnetic field is in a (110) plane, at an angle of 48° from the [100] axis. The solid line passing through the experimental points represents a least squares fit to the data, and, from its slope, the effective mass $m^* = 0.21m_0$ was obtained.

Since the small correction term $\exp \left(- \frac{4\pi^2 kT}{\hbar\omega_c} \right)$ contains the effective mass, it was necessary to obtain the final value of the effective mass through a series of iterations. The accuracy of the masses obtained in this manner is estimated to be 10%.

In Fig. 3, we show the effective masses of the carriers associated with the oscillations F_5 and F_6 , as a function of orientation, for the magnetic field in a (110) plane. The F_6 oscillations were only observed near the [100] axis and the effective mass associated with these carriers

could only be measured up to 24° from the $[100]$ axis. Similarly, the F_5 oscillations were not observed near the $[100]$ axis, disappearing with the appearance of the F_4 oscillations⁶ (which we did not observe). Thus, the effective mass of the carriers associated with these oscillations was only measured for angles greater than about 24° . In Fig. 3, we note that the mass associated with the F_5 oscillations varies considerably with orientation. For $\vec{H} \parallel [110]$, our value $m^* = (0.17 \pm 0.02)m_0$ is in good agreement with the value $m^* = 0.16m_0$, measured for this orientation by Ahn and Sellmyer.⁶ Although we did not measure m^* for $\vec{H} \parallel [111]$, our values of m^* for orientations close to the $[111]$ axis are in good agreement with the value $m^* = 0.21m_0$, obtained by Ahn and Sellmyer for $\vec{H} \parallel [111]$, from the temperature dependence of the magnetic susceptibility oscillations. (The upper point for the $[111]$ direction in Fig. 3 was obtained from the temperature dependence of the magnetic susceptibility oscillations, while the lower point was obtained from magneto-resistance oscillations.⁶)

D. Magnetic Field Dependence of the Amplitudes

It is well known that a study of the magnetic field dependence of the dHVA oscillations should allow one to determine the Dingle temperature T_D and, in addition, should indicate the presence of magnetic breakdown.¹⁶ In the present study, the magnetic field dependence of the attenuation oscillations was compared with Eq. (12) of ref. 14 to determine T_D . The field dependence of the F_6 oscillations was found to

be in good agreement with this equation with a value $T_D \sim 0.5K$, which was roughly independent of orientation. There was no evidence of magnetic breakdown up to the highest magnetic fields available (70 kOe).

For the F_5 oscillations, the situation was considerably more complicated. In Fig. 4, we show the field dependence of the attenuation amplitudes A , plotting the function $\frac{AH^{1/2}}{T} \sinh\left(\frac{2\pi^2 kT}{\hbar\omega_c}\right)$ against $1/H$, for two orientations of the magnetic field (The slope of such a plot is proportional to T_D . A reduction in slope at high values of H indicates magnetic breakdown). The upper plot is for the attenuation curve of Fig. 1, for which the magnetic field is in a (110) plane, 30° from the $[\bar{1}\bar{1}0]$ axis, while the lower plot is for \vec{H} in a (110) plane, 24° from the $[\bar{1}\bar{1}0]$ axis. From the linear portion of the lower curve, we find $T_D \sim 5K$, and the reduction in slope for high magnetic fields indicates magnetic breakdown. As can be seen in Fig. 4, the apparent breakdown field for this orientation is about 55 kOe. In contrast, the upper curve has a slightly positive slope, which, however, is probably connected with the slight scatter in the experimental points. Within experimental error we take the slope of the upper curve to be zero. Furthermore, there seems to be no sign of magnetic breakdown at high fields. The important point here is that both the apparent breakdown field, H_B , and T_D , calculated from the linear portion of the curve, seem to show a strong dependence upon

crystal orientation. Higgins and Marcus observed a similar behavior in connection with the "needles" in zinc.¹⁶ Moreover, they showed that, in the presence of magnetic breakdown, H_B and T_D must be determined from a simultaneous fit to the experimental data and that a determination of T_D from the linear portion of the curve may lead to gross errors. However, since a good Fermi surface model does not exist for AuSb_2 , the form of the magnetic breakdown correction cannot be determined and such a simultaneous fit is not possible. For this reason, we did not pursue our study of magnetic breakdown associated with the F_5 oscillations.

We note that Ahn and Sellmyer studied the magnetic breakdown of the F_5 oscillations for $\vec{H} \parallel [111]$, in both the high field magneto-resistance and the dHvA effect. In the former case they observed an apparent breakdown field $H_B = 70$ kOe, while in the latter case $H_B \lesssim 20$ kOe. They suggested an explanation of this puzzling fact in terms of two energy gaps, the upper one exclusively for the magneto-resistance oscillations and the lower one for the dHvA effect. However, it is known experimentally¹⁷ and theoretically¹⁸ that the apparent value of H_B determined from the magneto-resistance measurements moves to higher fields with decreasing relaxation time. This is not expected in equilibrium properties, such as the dHvA effect, according to a subsequent calculation.¹⁹ This may explain the apparent difference in the breakdown fields, without recourse to two different energy gaps.

ACKNOWLEDGMENTS - The authors would like to thank Prof. D.J. Sellmyer for providing the crystal used in these experiments. Furthermore, we would like to thank Profs. N.F. Oliveira, Jr. and C.J.A. Quadros for useful discussions.

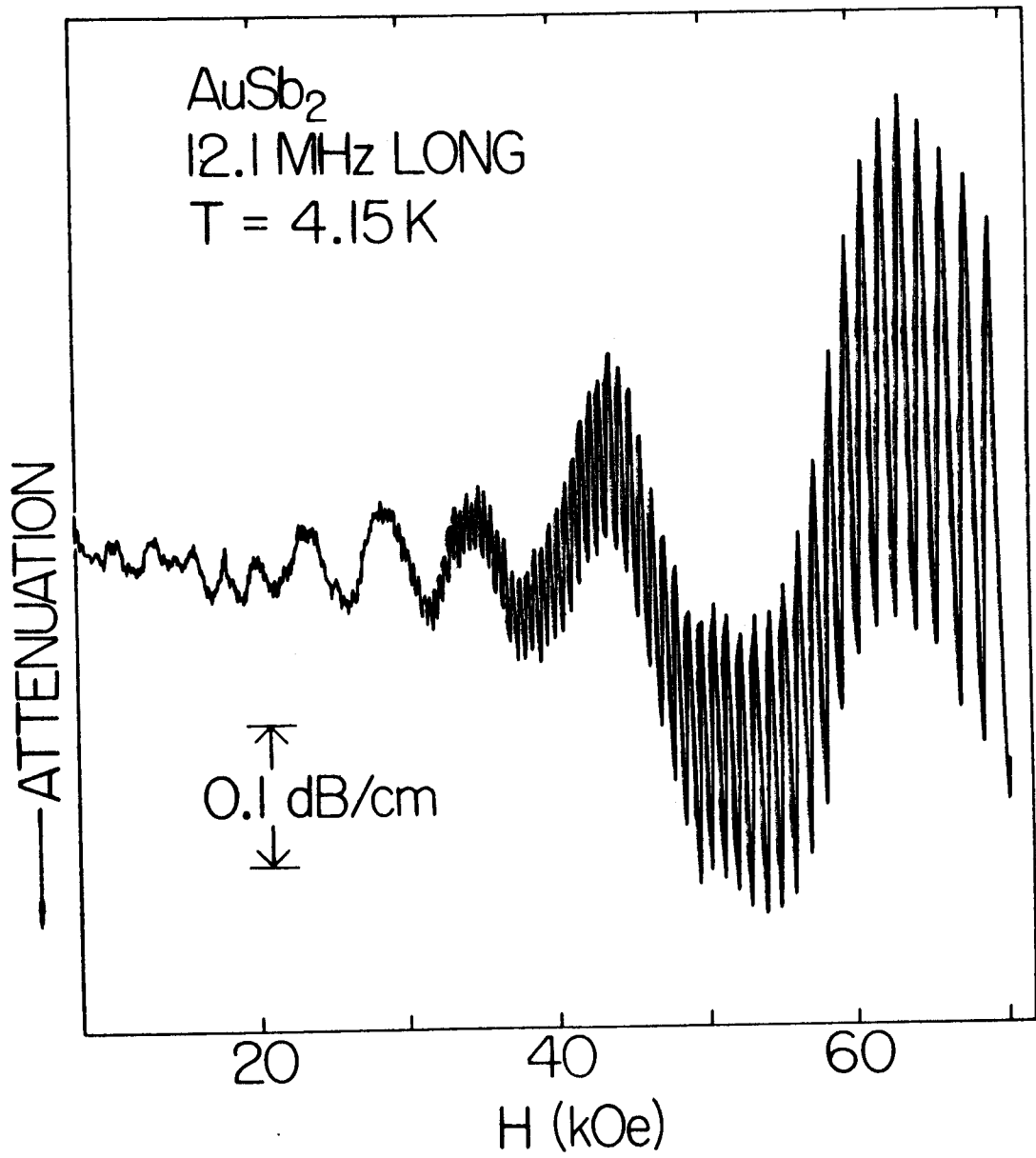
REFERENCES

1. PEARSON, W.B., Can. J. Phys. 42, 519 (1964)
2. MATHUR, M.P., MILLER, R.C.; & DAMON, D.H., Bull. Amer. Phys. Soc. 12, 1040 (1967).
3. EMTAGE, P.R.; DAMON, D.H.; MATHUR, M.P.; & MILLER, R.C., Phys. Rev. 180, 797 (1969).
4. AHN, J., & SELLMYER, D.J., Phys. Rev. B1, 1273 (1970).
5. BECK, A.; JAN, J.P.; PEARSON, W.B. & TEMPLETON, I.M., Phil. Mag. 8, 351 (1963).
6. AHN, J. & SELLMYER, D.J.- Phys. Rev. B1, 1285 (1970).
7. AHN, J., Ph.D. thesis, Massachusetts Institute of Technology, 1968 (unpublished).
8. JAN, J.P.; PEARSON, W.B., & SAITO, Y., Proc. Roy. Soc. (London) A297, 275 (1967).
9. TRUPELL, R.; ELBAUM, C., & CHICK, B.B., Ultrasonic Methods in Solid State Physics, p.53 Academic Press, New York (1969).
10. WYCKOFF, R.W.G., Crystal Structures, 2nd ed., Vol. 1, p. 346. John Wiley & Sons, Inc., New York (1963).
11. ALERS, G.A., In Physical Acoustics (Edited by W.P. Mason), Vol. 3, part B, p.1 Academic Press, New York (1965).
12. SHAPIRA, Y. & REED T.B., A.I.P. Conf. Proc. 5, 837 (1971).

13. KEESOM, P.H., & PEARLMAN, N., In Handbuch der Physik (Edited by S. Flügge), Vol. 14. Springer-Verlag, Berlin (1956).
14. REED, R.W. & BRICKWEDDE, F.G., Phys. Rev. B3, 1081 (1971).
15. SHAPIRA, Y., In Physical Acoustics (Edited by W.P. Mason), Vol. 5, p. 1. Academic Press, New York (1968).
16. HIGGENS, R.J., & MARCUS, J.A., Phys. Rev. 161, 589 (1967).
17. STARK, R.W., Phys. Rev. 135, A1698 (1964).
18. FALICOV, L.M., & SIEVERT, P.R., Phys. Rev. 138, A88 (1964).
19. FALICOV, L.M., & STACHOWIAK, H.- Phys. Rev. 147, 505 (1966).

FIGURE CAPTIONS

- Fig. 1 The magnetic field dependence of the attenuation oscillations for \vec{H} in a (110) plane, 30° from the $[\bar{1}10]$ axis.
- Fig. 2 The temperature dependence of the amplitude \underline{A} of the attenuation oscillations, for $H = 49.5$ kOe.
- Fig. 3 Angular dependence, in a (110) plane, of the effective masses of the carriers associated with the F_5 and F_6 .
- Fg. 4 Magnetic field dependence of the amplitude \underline{A} of the F_5 oscillations, for \vec{H} in a (110) plane. The points \bullet were obtained from the curve of Fig. 1, while $+$ were obtained for \vec{H} at 24° from the $[110]$ axis.



$$\ln \left[\frac{A}{T} \left(1 - e^{-\frac{4\pi^2 kT}{\hbar \omega_c}} \right) \right]$$

